August 27-31, 2023
FLORENCE - ITALY
ICWE 16
16th International Conference on Wind Engineering

Identification of aerodynamic admittance functions using an active turbulence grid

O. Kildal[1], Ø. W. Petersen[2], O. Øiseth[3]

[1]*NTNU, Trondheim, Norway, oddbjorn.kildal@ntnu.no*
[2]*NTNU, Trondheim, Norway, oyvind.w.petersen@ntnu.no*
[3]*NTNU, Trondheim, Norway, ole.oiseth@ntnu.no*

SUMMARY
All long-span bridges are continuously subject to loading from turbulent winds. How the turbulent winds transfer forces onto a bridge cross-section depends on the aerodynamic admittance functions of the cross-section and the turbulence. A pressure tap model was built to acquire the necessary data to deduce 3D one-wavenumber aerodynamic admittance functions for a twin-deck bridge section under various turbulent flows. Homogeneous freestream turbulence was generated by an active turbulence grid upstream of the section model while a cobra probe in front of the section model was used to measure the flow properties. Three different turbulent flows were applied during the testing by operating the active grid in different ways. Aerodynamic admittance functions were estimated using both the auto-spectrum method and the cross-spectrum method. It was observed that the aerodynamic admittance functions changed with changing turbulence and that the cross-spectrum method for estimating aerodynamic admittance functions is flawed for stochastic flow.

Keywords: Active grid, twin deck, aerodynamic admittance

1 INTRODUCTION

Aerodynamic admittance functions (AAFs) are functions of frequency that map turbulent winds to buffeting forces. For bluff bodies like bridges that are not streamlined and always exhibit flow separation, there are no analytic AAFs. Therefore, we try to estimate the AAFs for bridge cross-sections empirically by conducting wind tunnel experiments.

Various approaches exist to generate turbulence in wind tunnels. A passive grid and spires were used by Counihan (1969) to create up to around 10% turbulence intensity. Makita (1991) achieved turbulence intensities above 16% using an active turbulence grid while retaining homogeneity and isotropy. Knebel et al. (2011) reached turbulence intensities higher than 25% using an active turbulence grid. Active turbulence grids can produce high turbulence intensities and large integral length scales, as shown by Makita (1991) and Knebel et al. (2011). Li et al. (2018) clarified the meaning of the 2D AAF, the 3D one-wavenumber AAF, and the 3D two-wavenumber AAF. The auto-spectrum method uses empirical turbulence and force auto-spectrums to identify AAFs where the horizontal and the vertical turbulence AAFs are assumed to be equal. The cross-spectrum method uses empirical auto and cross spectrums to identify AAFs where the horizontal and the vertical turbulence AAFs are estimated separately and not assumed to be equal.

The present study investigates the effect of turbulence on 3D one-wavenumber AAFs.

2 EXPERIMENTAL SET-UP

Wind tunnel testing was conducted with an active turbulence grid, as shown in Fig. 1 a), a pressure tap section model mounted in a forced vibration rig (Siedziako et al., 2017), and two cobra probes, as portrayed in Fig. 1 b).

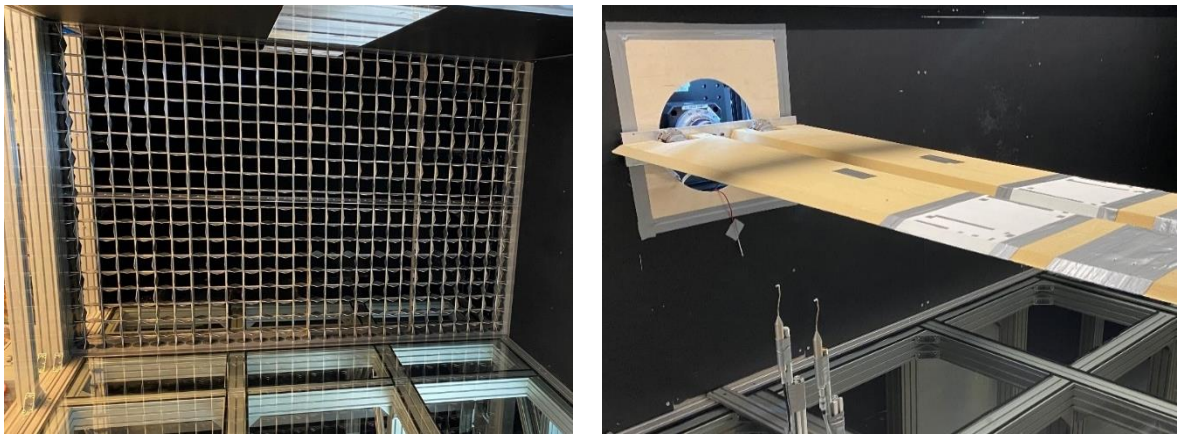

a) Active turbulence grid in the open state. b) Section model with pressure taps.

Figure 1. Experimental set-up.

The middle section of the pressure tap model is a 3D-printed part with pressure measurements in six different correlation lines.

3 WIND TUNNEL EXPERIMENTS

Wind tunnel experiments were conducted to investigate aerodynamic admittance functions (AAFs) in an active grid-generated turbulent flow.

3.1 Flow cases

Table 1 shows the turbulence characteristics for the three flow cases used in the wind tunnel testing. The integral length scales were deduced by fitting von Karman spectra to the observed auto-spectral densities of the flow.

Table 1. Grid cases and flow properties.

Grid case	U [m/s]	I_u	xL_u [m]	R_{uw}
Still open	9.1	0.02	-	-
Grid case 1	9.0	0.10	0.247	0.000
Grid case 2	9.0	0.16	0.570	0.000

3.2 Admittance functions using the auto-spectrum method

AAFs estimated by the auto-spectrum method (ASM) assume the AAFs for horizontal and vertical turbulence are the same. The ASM AAF for lift forces is given in Eq. (1).

$$|A_L|^2 = \frac{S_L}{(\frac{1}{2}\rho BU)^2(a_L{}^2 S_u + b_L{}^2 S_w)}, a_L = 2C_L, b_L = (dC_L + \frac{D}{B}C_D) \quad (1)$$

Fig. 2 shows the ASM AAFs deduced for wind speeds around 9 m/s plotted against Sears function as a reference. The figure shows that the ASM AAFs increase with increasing turbulence for low reduced frequencies. For high reduced frequencies, the ASM AAFs

decrease with increasing turbulence. It is generally observed that the ASM AAFs are not invariant with changing flow properties.

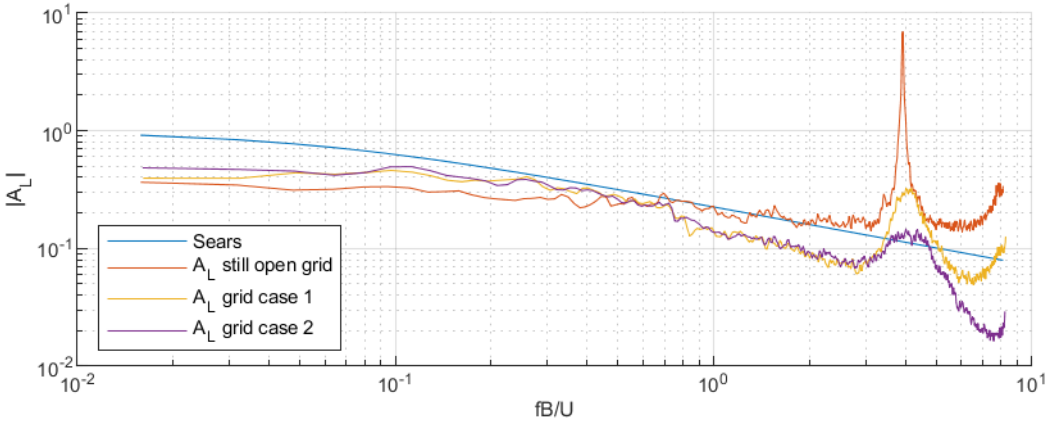

Figure 2. ASM AAFs for lift with wind speed of about 9 m/s and different grid cases.

The peaks observed around 48 Hz are because of vortex shedding.

3.3 Admittance functions using the cross-spectrum method

AAFs estimated by the cross-spectrum method (CSM) can be used to avoid the assumption that the AAFs for horizontal and vertical turbulence are the same. The CSM AAFs for lift are given in Eq. (2).

$$|A_{Lu}| = \left| \frac{S_w S_{Lu} - S_{uw} S_{Lw}}{\frac{1}{2}\rho B U a_L (S_u S_w - S_{wu} S_{uw})} \right|, |A_{Lw}| = \left| \frac{S_u S_{Lw} - S_{uw} S_{Lu}}{\frac{1}{2}\rho B U b_L (S_u S_w - S_{wu} S_{uw})} \right| \quad (2)$$

Fig. 3 shows CSM AAFs for horizontal turbulence at about 9 m/s wind speed and Sears function as a reference. For high reduced frequencies, the CSM AAFs for the still open grid case and grid case 1 are a bit higher than for grid case 2.

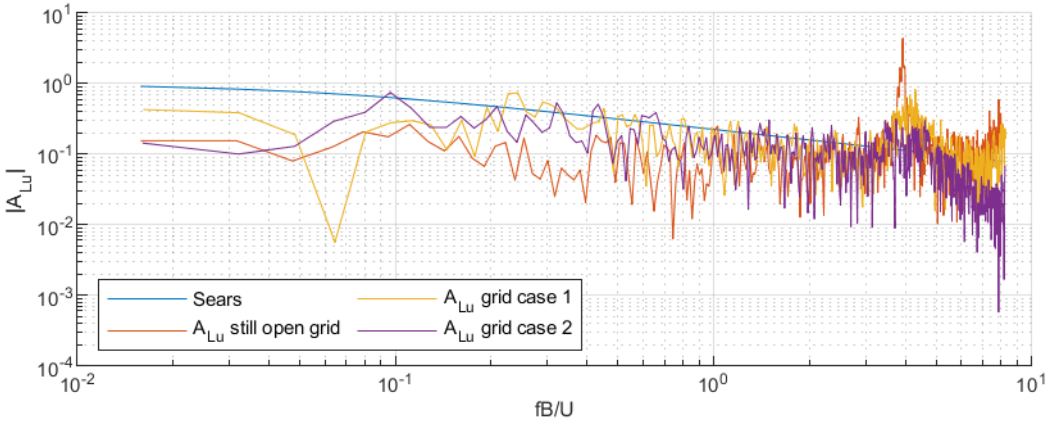

Figure 3. Horizontal turbulence CSM AAFs for lift with wind speed of about 9 m/s and different grid cases.

Fig. 4 shows CSM AAFs for vertical turbulence at about 9 m/s wind speed and Sears function as a reference. It is seen the CSM AAFs decrease with turbulence for high reduced frequencies.

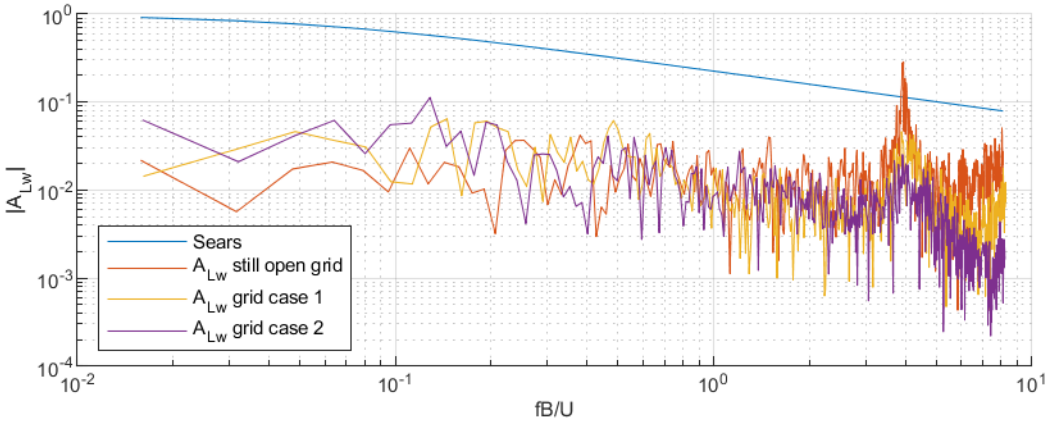

Figure 4. Vertical turbulence CSM AAFs for lift with wind speed of about 9 m/s and different grid cases.

It is observed that the CSM AAFs seem to be inaccurate as they deviate very much from the Sears function. However, they are in the same order of magnitude as in Yan et al. (2018). Consider the approximation of the vertical turbulence CSM AAF in Eq. (3).

$$|A_{Lw}| = \left| \frac{S_u S_{Lw} - S_{uw} S_{Lu}}{\frac{1}{2}\rho B U b_L (S_u S_w - S_{wu} S_{uw})} \right| \overset{S_{uw} \approx 0}{\approx} \left| \frac{S_{Lw}}{\frac{1}{2}\rho B U b_L S_w} \right| = \left| \frac{Coh_{Lw}\sqrt{S_L S_w}}{\frac{1}{2}\rho B U b_L S_w} \right| = \left| \frac{Coh_{Lw}\sqrt{S_L}}{\frac{1}{2}\rho B U b_L \sqrt{S_w}} \right| \tag{3}$$

Since Coh_{Lw} depends on the separation between the cobra probe and the section model, this affects the identification procedure and makes the CSM flawed for stochastic flow.

4 CONCLUSION

The aerodynamic admittance functions (AAFs) are observed to vary with turbulence for the considered cross-section. The AAFs seem to decrease with increasing turbulence for high reduced frequencies. Some challenges in estimating AAFs are observed.

ACKNOWLEDGEMENTS

The authors gratefully acknowledge the Norwegian Public Roads Administration, for the general research support within the innovative E39 Coastal Highway Route project.

REFERENCES

Counihan, J. (1969). An improved method of simulating an atmospheric boundary layer in a wind tunnel. *Atmospheric Environment (1967)*, *3*(2), 197–214.

Hideharu, M. (1991). Realization of a large-scale turbulence field in a small wind tunnel. *Fluid Dynamics Research*, *8*(1–4), 53.

Knebel, P., Kittel, A., & Peinke, J. (2011). Atmospheric wind field conditions generated by active grids. *Experiments in Fluids*, *51*(2), 471–481.

Li, S., Li, M., & Larose, G. L. (2018). Aerodynamic admittance of streamlined bridge decks. *Journal of Fluids and Structures*, *78*, 1–23.

Siedziako, B., Øiseth, O., & Rønnquist, A. (2017). An enhanced forced vibration rig for wind tunnel testing of bridge deck section models in arbitrary motion. *Journal of Wind Engineering and Industrial Aerodynamics*, *164*, 152–163.

Yan, L., Zhu, L.-D., & Flay, R. G. J. (2018). Identification of aerodynamic admittance functions of a flat closed-box deck in different grid-generated turbulent wind fields. *Advances in Structural Engineering*, *21*(3), 380–395.